Single-Carrier 2.5-Tb/s Transmission Using CSRZ-OTDM with 8×4 Digital Calibrator

Hiroshi Yamazaki(1,2), Masanori Nakamura(1), Yoshihiro Ogiso(3), Josuke Ozaki(3), Takayuki Kobayashi(1), Toshikazu Hashimoto(2), and Yutaka Miyamoto(1)

(1) NTT Network Innovation Labs., NTT Corporation, 1-1 Hikari-no-oka, Yokosuka, Japan, hrsh.yamazaki@ntt.com
(2) NTT Device Technology Labs., NTT Corporation, 3-1 Morinosato Wakamiya, Atsugi, Japan
(3) NTT Device Innovation Center, NTT Corporation, 3-1 Morinosato Wakamiya, Atsugi, Japan

Abstract *We demonstrate a 224-GBaud CSRZ-OTDM optical transmitter achieving net bit rates of 2.59 Tb/s/λ back-to-back and 2.52 Tb/s/λ after 80-km SSMF transmission. An 8×4 digital calibrator effectively compensates for spurious distortions. ©2023 The Author(s)*

Introduction

Toward more efficient accommodation of rapidly growing data traffic, higher per-wavelength data rates are being pursued by researchers in the field of digital coherent transmission technologies. Fig. 1 summarizes recent results showing net bit rates exceeding 1.5 Tbps, each demonstrated with a single continuous-wave (CW) transmission light source. The bit rates up to 2.11 Tb/s were achieved by using two SiGe digital-to-analog converters (DACs) interleaved in the baseband (BB) in each signaling dimension [1-4], while those up to 1.96 Tbps were reached with a single SiGe DAC in each [5–10]. Transmitters with CMOS DACs and intermediate-frequency-involving (IFI) interleaving technologies have also been explored, such as an optical phase-interleaving transmitter operating at 1.68 Tbps [11] and electronic frequency-interleaving one at 1.58 Tbps [12]. In principle, IFI interleaving is promising for achieving even higher bit rates as it extends the available signal bandwidth beyond the DACs' analog bandwidth. On the other hand, recent SiGe DACs have shown excellent performance at 1 sample/symbol (Sa/sym) as their analog bandwidths exceeds their Nyquist frequencies [5–10].

In this study, we demonstrate a way to combine the benefits of the IFI interleaving and 1-Sa/sym DACs. We use optical time-division multiplexing (OTDM) with carrier-suppressed-return-to-zero (CSRZ) pulses, which multiplexes two single-carrier signals, each generated by 1-Sa/sym DACs, to double the symbol rate with relatively simple optics and a high spectral efficiency [13]. To enhance the signal quality, we utilize an 8×4 digital calibrator to compensate for the distortions caused by spurious components and other imbalances in the transmitter. In an experiment using 112-GSample/sec (GSa/s) SiGe DACs and InP modulators, we demonstrate record CW-sourced single-carrier net bit rates of

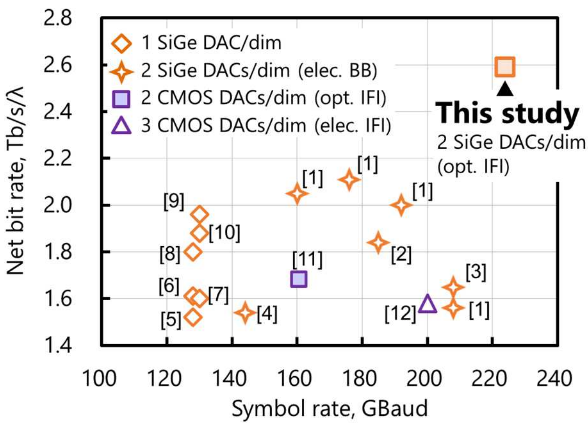

Fig. 1: Overview of recently reported single-carrier optical transmitters operating at net >1.5 Tb/s.

2.59 Tb/s and 2.52 Tb/s in back-to-back and over-80-km standard single-mode fiber (SSMF) transmission, respectively.

Principle

The configuration of the CSRZ-OTDM transmitter (single polarization) for generating 2B-Baud signals is shown in Fig. 2(a). We use a CW laser oscillating at a frequency of f_c and a single null-biased Mach-Zehnder modulator (MZM) driven at a frequency of $B/2$ as a CSRZ carver [14]. The carver's output is sent to a delayed dual in-phase-and-quadrature modulator (D2IQM), which has two IQMs connected in parallel with a relative time delay of $1/(2B)$. The D2IQM is driven by B-Baud sub-signals generated by four DACs corresponding to the I and Q components of the two sub-channels, each operating at 1 Sa/sym. The digital signal processor (DSP) before the DACs is explained later. Fig. 2(b) is a time-domain diagram of the CSRZ-OTDM signaling [13]. The symbol timings of the two sub-channels alternate, and each coincides with the extinction of the CSRZ waveform of the other sub-channel, avoiding inter-symbol interference. As shown at the top of Fig. 2(c), the CSRZ wave input to the D2IQM has two main frequency components at

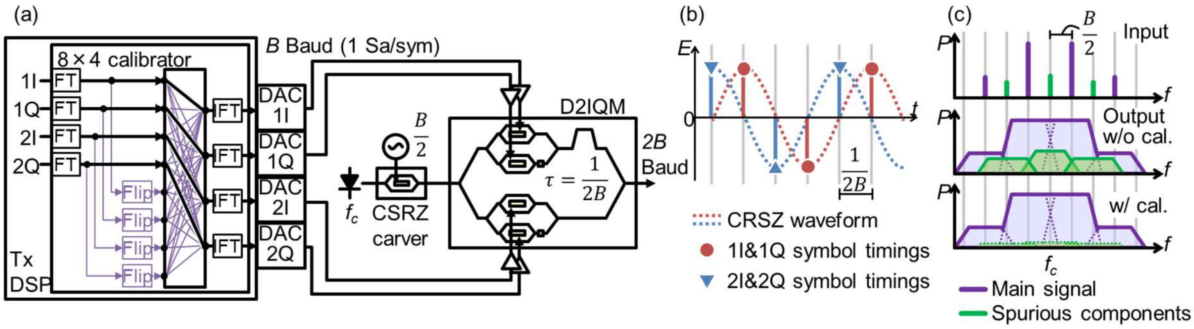

Fig. 2: (a) Transmitter configuration. (b) Time-domain diagram of CSRZ-OTDM. (c) Schematic spectrum of input waveform to D2IQM (top) and those of output signal without (middle) and with (bottom) calibrator.

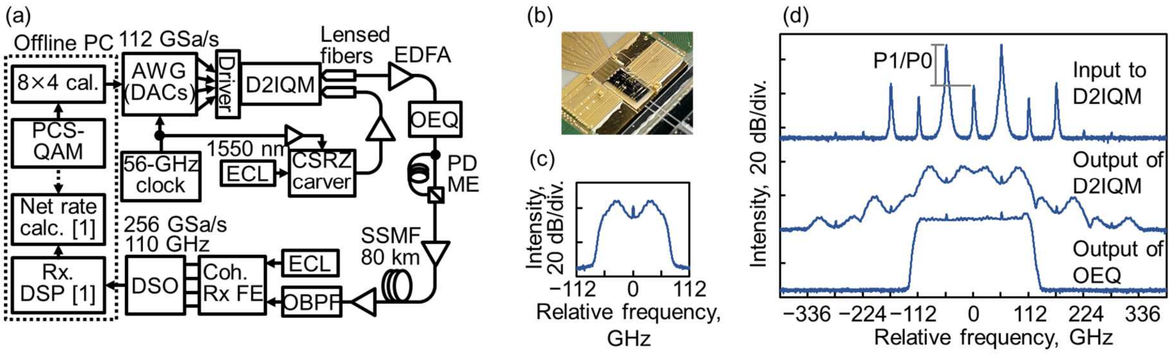

Fig. 3: (a) Experimental setup. (b) D2IQM chip on the evaluation board. (c) Output optical spectrum of D2IQM with CW input. (d) Optical spectra measured at different points of the setup.

$f_c \pm B/2$. Thus, the signal power of the output from the D2IQM is mostly concentrated within the Nyquist frequency of $f_c \pm B$, as shown in the middle and at the bottom of Fig. 2(c). As such, CSRZ-OTDM is a frequency-efficient way of doubling the symbol rate with relatively simple optics. In a practical implementation, however, the CSRZ wave also has some spurious frequency components at f_c and $f_c \pm B$ due to imbalances in the carver, as shown at the top of Fig. 2(c). If we simply drive the D2IQM with B-Baud sub-signals independent of each other, namely, without any calibration, the D2IQM's output would be contaminated by signals convoluted to the spurious components, as shown in the middle of Fig. 2(c). Furthermore, imbalances between the two IQMs in the D2IQM would also degrade the signal quality. To compensate for those impairments, we use a frequency-domain 8×4 digital calibrator in the DSP, as shown in Fig. 2(a). The calibrator shares the basic structure of the digital spectral weaver (DSW) we used in [11]; it generates signals to be sent to the DACs from four inputs and their spectrally flipped copies. The differences are that now the inputs are 1-Sa/sym sub-symbol sequences instead of spectral slices of the target signal. Since the calibrator compensates only for hardware imperfections, it makes only minor changes to those sub-symbol sequences, keeping the merit of 1-Sa/sym operation.

Experiment

We performed 224-GBaud digital coherent transmissions with the setup shown in Fig. 3(a). An offline PC and a 112-GSa/s SiGe arbitrary waveform generator (AWG, Keysight M8199A) were used to emulate a DSP interfaced with the DACs. The D2IQM chip (2.5×5.0 mm2) was fabricated by using the n-p-i-n InP modulator platform [15] and was mounted on an evaluation board with a four-channel driver amplifier, as shown in Fig. 3(b). A pair of spherical lensed fibers fixed to moving stages were used to optically access the D2IQM, whose optical insertion loss at 1550 nm with minimum-loss biases was 6.0 dB including fiber coupling losses. As shown in Fig. 3(c), the output optical spectrum of the D2IQM with CW input had a gullwing shape due to the strong peaking of the driver [16]. As the transmission light source and the local oscillator, we used two separate 1550-nm CW external-cavity lasers (ECLs) with a linewidth of ~10 kHz. The CSRZ carver, which was also fabricated on the basis of the InP platform, was driven by a 56-GHz clock signal, which was split from the clock to drive the AWG. The output from the carver was amplified by an erbium-doped fiber amplifier (EDFA) to +18 dBm, and that from the D2IQM was also amplified by another EDFA before being input to an optical equalizer (OEQ) followed by a polarization-division-multiplexing emulator (PDME) with a 65.7-ns (~14.7k

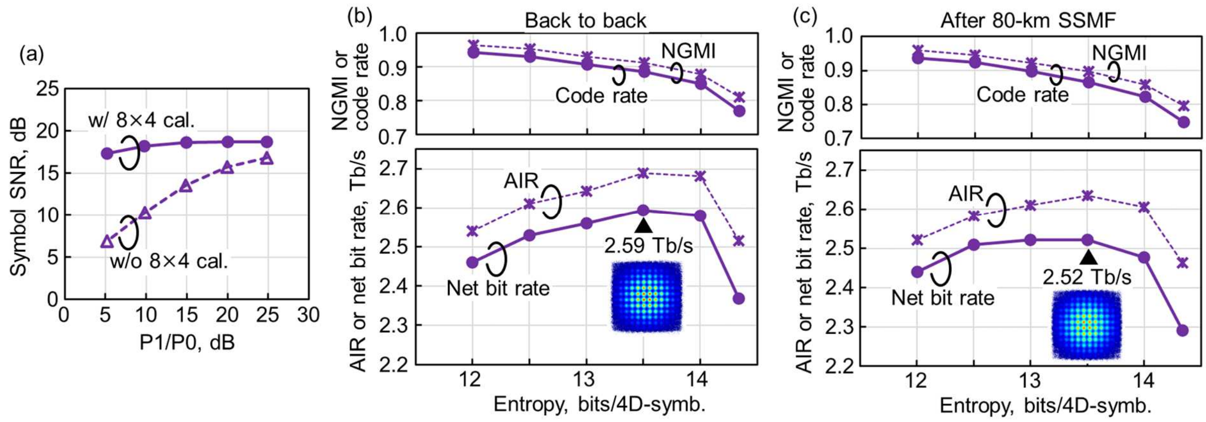

Fig. 4: (a) Symbol SNR vs. P1/P0. (b) NGMI, code rate, AIR, and net data rate vs. entropy at back-to-back. (c) Those after 80-km SSMF transmission.

symbols) delay line. The optical signal spectra measured at the input and output of the D2IQM and the output of the OEQ are shown in Fig. 3(d), where the horizontal axis is the frequency relative to the optical carrier frequency. The input to the D2IQM (Fig. 3(d), top) had some spurious components at 0 and ±112 GHz along with the main components at ±56 GHz. The power ratio of the main to the largest (center) spurious component, P1/P0, was varied by controlling the bias of the carver to test the calibrator's performance, and finally set to 25 dB for the transmission demonstration. The output spectrum of the D2IQM (Fig. 3(d), middle) corresponds to a convolution of those shown in Fig. 3(c) and at the top of Fig. 3(d). This twin-gullwing spectrum was flattened by the OEQ (Fig. 3(d), bottom). After transmission over 80-km SSMF, EDFAs, and an optical band-pass filter (OBPF), the PDM signal was received by a coherent receiver frontend followed by a 256-GSa/s 110-GHz digital storage oscilloscope (DSO). In the offline DSP, we first optimized the calibrator's coefficients by using test signals. Then, we transmitted 224-GBaud probabilistically constellation-shaped 144-level quadrature amplitude modulation (PCS-144QAM) signals each with a length of ~3×10^5 and a pilot overhead (OH) of 0.79%. To avoid overfitting, the test and QAM signals were generated on the basis of a random number generator (Mersenne Twister) with different seeds. The receiver-side analyses were performed in a similar manner as we did in [1]; the captured signals were resampled to 2 Sa/sym before being demodulated by using a frequency-domain 8×2 adaptive equalizer with an FFT block size of 8,192 (corresponding to 4,096 taps at a time domain T/2-spaced equalizer) with a pilot-based digital phase-locked loop. The net bit rate was calculated through a code-rate adaptation method based on a family of DVB-S2 low density parity check (LDPC) codes [17] with a puncturing method [18] to enable rate-adaptive coding [19] assuming an outer hard-decision forward error correction code with a code rate of 0.9922 and bit-error-rate threshold of 5×10−5 [20].

Fig. 4(a) shows the symbol signal-to-noise ratio (SNR) of the PCS-144QAM signal with an entropy of 13.0 bits/4D-symbol at various P1/P0 with and without the 8×4 calibrator. An SNR gain of ~2 dB, which corresponds to a bit-rate gain of ~300 Gb/s in this case, was obtained by the calibrator at P1/P0 of 25 dB, and the gain significantly increased as P1/P0 decreased. Figs. 4(b) and (c) show the normalized generalized mutual information (NGMI), required code rate, achievable information rate (AIR), and net bit rate as a function of the entropy for the back-to-back and over-80-km transmission cases, respectively. The AIR and net bit rate were calculated by C={H−(1−R)×16}/1.0079×0.224, where C is the AIR or net bit rate, H is the entropy per each 4D symbol, and R is the NGMI or code rate. Maximum net bit rates of 2.59 Tb/s for back-to-back and 2.52 Tb/s for over-80-km-SSMF transmissions were achieved both at an entropy of 13.5 bits/4D-symbol.

Conclusion

We demonstrated the first >2.5-Tb/s CW-sourced single-carrier transmission by using a 224-GBaud CSRZ-OTDM transmitter with 112-GSa/s 1-Sa/sym SiGe DACs and InP modulators. An 8×4 digital calibrator significantly enhanced the performance and tolerance to the spurious in the CSRZ wave. This technology is promising for achieving multi-terabit/λ optical transmission with a moderate hardware complexity.

References

[1] M. Nakamura, M. Nagatani, T. Jyo, F. Hamaoka, M. Mutoh, Y. Shiratori, H. Wakita, T. Kobayashi, H. Takahashi, and Y. Miyamoto, "Over 2-Tb/s Net Bitrate Single-carrier Transmission Based on >130-GHz-Bandwidth InP-DHBT Baseband Amplifier Module," presented at *European Conference on Optical*

Communication (ECOC'22), Basel, Switzerland, 2022, paper Th3C.1.

[2] M. Mardoyan, S. Almonacil, F. Jorge, F. Pittalà, M. Xu, B. Krueger, F. Blache, B. Duval, L. Chen, Y. Yan, X. Ye, A. Ghazisaeidi, S. Rimpf, Y. Zhu, J. Wang, M. Goix, Z. Hu, M. Duthoit, M. Gruen, X. Cai, and J. Renaudier, " First 260-GBd Single-Carrier Coherent Transmission over 100 km Distance Based on Novel Arbitrary Waveform Generator and Thin-Film Lithium Niobate I/Q Modulator," presented at *European Conference on Optical Communication (ECOC'22)*, Basel, Switzerland, 2022, paper Th3C.2.

[3] M. Nakamura, H. Taniguchi, S. Yamamoto, F. Hamaoka, M. Nagatani, T. Jyo, M. Mutoh, Y. Shiratori, H. Wakita, T. Kobayashi, H. Takahashi, and Y. Miyamoto, "Beyond 200-GBd QAM Signal Detection Based on Trellispath-limited Sequence Estimation Supporting Soft-decision Forward Error Correction," presented at *Optical Fiber Communication Conference (OFC'23)*, San Diego, CA, USA, 2023, paper M1F.2.

[4] F. Hamaoka, M. Nakamura, M. Takahashi, T. Kobayashi, and Y. Miyamoto, " 173.7-Tb/s Triple-Band WDM Transmission using 124-Channel 144-GBaud Signals with SE of 9.33 b/s/Hz," presented at *Optical Fiber Communication Conference (OFC'23)*, San Diego, CA, USA, 2023, paper Th3F.2.

[5] F. Buchali, V. Aref, M. Chagnon, K. Schuh, H. Hettrich, A. Bielik, L. Altenhain, M. Guntermann, R. Schmid, and M. Möller, "1.52 Tb/s Single Carrier Transmission Supported by a 128 GSa/s SiGe DAC," presented at *Optical Fiber Communication Conference (OFC'20)*, San Diego, CA, USA, 2020, paper Th4C.2, DOI: 10.1364/OFC.2020.Th4C.2

[6] V. Bajaj, F. Buchali, M. Chagnon, S. Wahls and V. Aref, "Single-channel 1.61 Tb/s Optical Coherent Transmission Enabled by Neural Network-Based Digital Pre-Distortion," presented at *European Conference on Optical Communication (ECOC'20)*, Brussels, Belgium, 2020, paper Tu1D.5, DOI: 10.1109/ECOC48923.2020.9333267

[7] F. Pittalà, R-P. Braun, G. Boecherer, P. Schulte, M. Schaedler, S. Bettelli, S. Calabrò, M. Kuschnerov, A. Gladisch, F-J. Westphal, C. Xie, R. Chen, Q. Wang, and B. Zheng, "Single-Carrier Coherent 930G, 1.28T and 1.60T Field Trial," presented at *European Conference on Optical Communication (ECOC'21)*, Bordeaux, France, 2021, paper, Th2C1.1, DOI: 10.1109/ECOC52684.2021.9605966

[8] M. Nakamura, T. Kobayashi, F. Hamaoka, and Y. Miyamoto, "High Information Rate of 128-GBaud 1.8-Tb/s and 64-GBaud 1.03-Tb/s Signal Generation and Detection Using Frequency-Domain 8×2 MIMO Equalization," *in Proceedings of Optical Fiber Communication Conference (OFC'22)*, San Diego, CA, USA, 2022, paper M3H.1

[9] M. Xu, Y. Zhu, F. Pittalà, J. Tang, M. He, W. C. Ng, J. Wang, Z. Ruan, X. Tang, M. Kuschnerov, L. Liu, S. Yu, B. Zheng, and X. Cai, "Dual-polarization thin-film lithium niobate in-phase quadrature modulators for terabit-per-second transmission," *Optica,* vol. 9, no. 1, pp. 61-62, 2022, DOI: 10.1364/OPTICA.449691

[10] F. Pittalà, R-P. Braun, G. Böcherer, P. Schulte, M. Schaedler, S. Bettelli, S. Calabrò, M. Kuschnerov, A. Gladisch, F-J. Westphal, C. Xie, R. Chen, Q. Wang, and B. Zheng, "1.71 Tb/s Single-Channel and 56.51 Tb/s DWDM Transmission Over 96.5 km Field-Deployed SSMF," *IEEE Photonics Technology Letters*, vol. 34, no. 3, pp. 157-160, 2022, DOI: 10.1109/LPT.2022.3142538

[11] H. Yamazaki, Y. Ogiso, M. Nakamura, T. Jyo, M. Nagatani, J. Ozaki, T. Kobayashi, T. Hashimoto, and Y. Miyamoto, "Transmission of 160.7-GBaud 1.64-Tbps Signal Using Phase-Interleaving Optical Modulator and Digital Spectral Weaver," *Journal of Lightwave Technology*, *Early Access*, 2023, DOI: 10.1109/JLT.2023.3236350.

[12] X. Chen, G. Raybon, D. Che, J. Cho and K. W. Kim, "Transmission of 200-GBaud PDM Probabilistically Shaped 64-QAM Signals Modulated via a 100-GHz Thin-film LiNbO3 I/Q Modulator," *in Proceedings of Optical Fiber Communication Conference (OFC'21),* San Francisco, CA, USA, 2021, paper F3C.5, DOI: 10.1364/OFC.2021.F3C.5

[13] H. Yamazaki, A. Sano, M. Nagatani, and Y. Miyamoto, "Single-carrier 1-Tb/s PDM-16QAM transmission using high-speed InP MUX-DACs and an integrated OTDM modulator," *Optics Express*, vol. 23, no. 10, pp. 12866-12873, 2015, DOI: 10.1364/OE.23.012866.

[14] Y. Miyamoto, A. Hirano, K. Yonenaga, A. Sano, H. Toba, K. Murata, and O. Mitomi, "320Gbit/s (8 x 40 Gbit/s) WDM transmission over 367 km with 120 km repeater spacing using carrier-suppressed return-to-zero format," *Electronics Letters*, vol. 35, no. 23, pp. 2041-2042, 1999, DOI: 10.1049/EL:19991373

[15] Y. Ogiso, J. Ozaki, Y. Ueda, H. Wakita, M. Nagatani, H. Yamazaki, M. Nakamura, T. Kobayashi, S. Kanazawa, Y. Hashizume, H. Tanobe, N. Nunoya, M. Ida, Y. Miyamoto, and M. Ishikawa, "80-GHz Bandwidth and 1.5-V $V\pi$ InP-Based IQ Modulator," *Journal of Lightwave Technology*, vol. 38, no. 2, pp. 249-255, 2020, DOI: 10.1109/JLT.2019.2924671

[16] J. Ozaki, Y. Ogiso, Y. Hashizume, H. Yamazaki, K. Nagashima, and M. Ishikawa, "Coherent Driver Modulator With Flexible Printed Circuit RF Interface for 128-Gbaud Operations," *Photonics Technology Letters*, vol. 34, no. 23, pp. 1289-1292, 2022, DOI: 10.1109/LPT.2022.3212678.

[17] ETSI, "Digital Video Broadcasting (DVB); Second generation framing structure, channel coding and modulation systems for Broadcasting, Interactive Services, News Gathering and other broadband satellite applications, " EN 302 307-1, v.1.4.1, 2014.

[18] T. Yoshida, M. Karlsson, and E. Agrell, "Efficient Offline Evaluation of FEC Codes Based on Captured Data with Probabilistic Shaping," in *Proceedings Optical Fiber Communication Conference (OFC'18)*, San Diego, CA, USA, 2018, M4E.5., DOI: 10.1364/OFC.2018.M4E.5.

[19] A. Ghazisaeidi, L. Schmalen, I. Fernandez de Jauregui Ruiz, P. Tran, C. Simonneau, P. Brindel, and G. Charlet, "Transoceanic Transmission Systems Using Adaptive Multirate FECs," *Journal of Lightwave Technology*, vol. 33, no. 7, pp. 1479-1487, 2015, DOI: 10.1109/JLT.2015.2399174.

[20] D. S. Millar, R. Maher, D. Lavery, T. Koike-Akino, M. Pajovic, A. Alvarado, M. Paskov, K. Kojima, K. Parsons, B. C. Thomsen, S. J. Savory, and P. Bayvel, "Design of a 1 Tb/s Superchannel Coherent Receiver," *Journal of Lightwave Technology*, vol. 34, no. 6, pp. 1453-1463, 2016, DOI: 10.1109/JLT.2016.2519260.